PRIMORDIAL NUCLEOSYNTHESIS

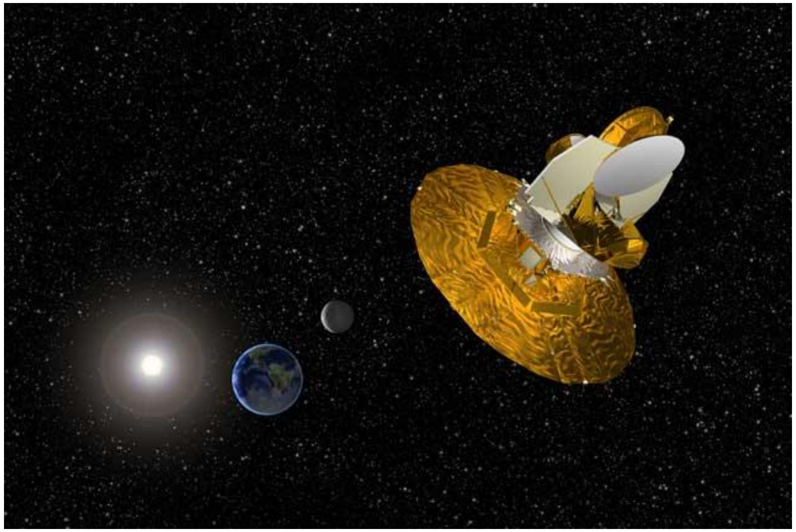

Hot "Big Bang" Cosmology MODEL

- Adiabatically expanding,
- Monotonically cooling
- Undergoing a series of phase transitions
- Structure defined by RW metric and Friedmann equations

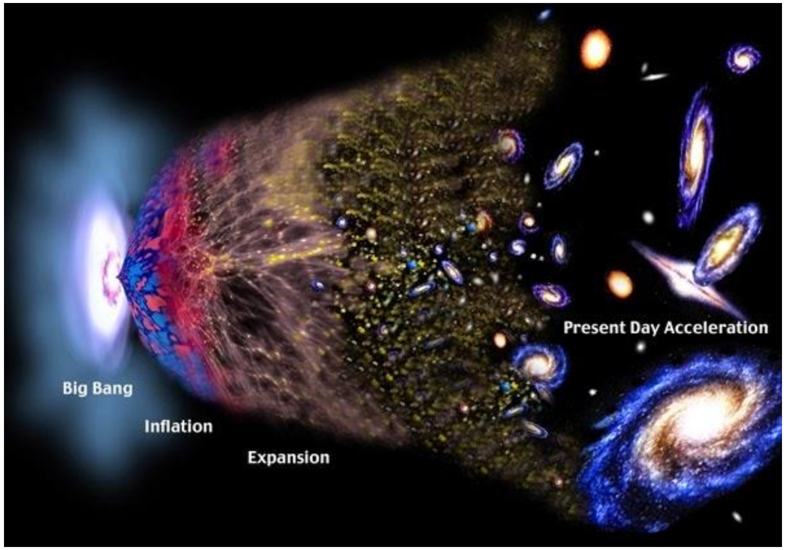

Standard Big Bang cosmology pillars

- Hubble flow
  - supported by recesion of galaxies
- Primordial nucleosynthesis
  - supported by primordial abundances (Y_p)
- Cosmic microwave background
  - supported by the 2.7K radiation

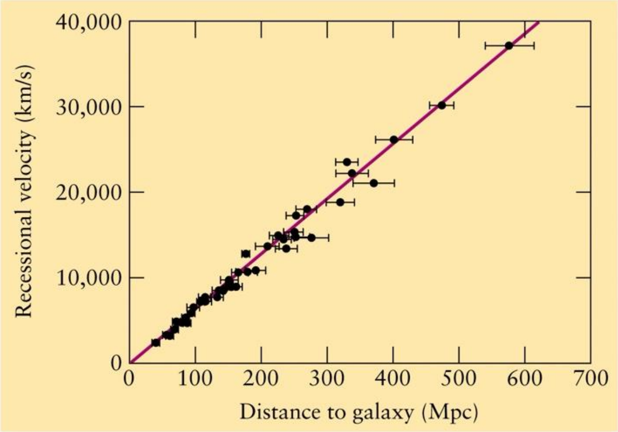

Universe timeline

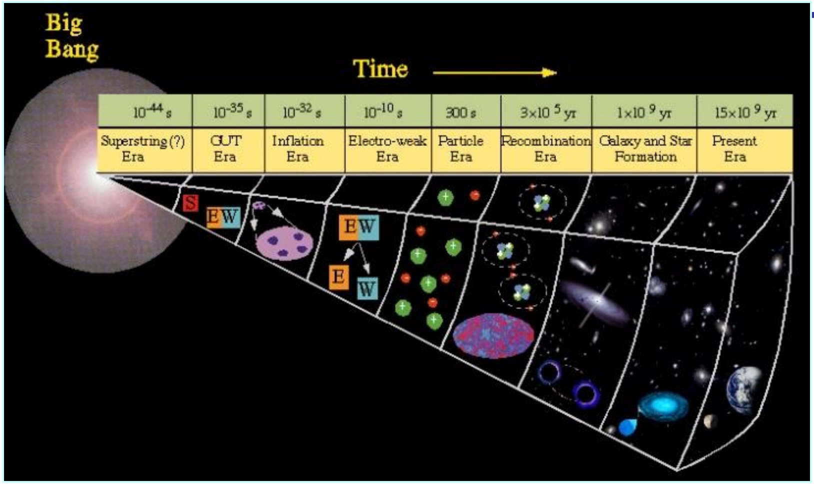

Event	t_U	T_U	Notes
Planck Time	10^{-43} s	10^{19} GeV	GR breaks down
Strong Force	10^{-36} s	10^{14} GeV	GUT
Inflation Era	$10^{-36} - 10^{-32}$ s		
Weak Force	10^{-12} s		
Quark-Hadron Transition	10^{-5} s	300 MeV	Hadrons form
Lepton Era	$10^{-5} - 10^{-2}$ s	130 Mev – 500 keV	$e^+ - e^-$ annihilation
Nucleosynthesis	$10^{-2} - 10^{2}$ s	~ 1 MeV	Light elements form
Radiation-Matter Equality	50,000 yrs ($z = 3454$)	9400 K	
Recombination	372,000 yrs ($z = 1088$)	2970 K (0.3 eV)	CMB
Reionization	$\sim 10^{8}$ yrs ($z = 6 - 20$)	50 K	
Galaxy Formation	Reionization til now	50-2.7 K	
Present Day	13.7 Gyrs	2.7 K ($\sim 10^{-4}$ eV)	

UAM UNIVERSIDAD AUTONOMA DE MADRID

Outline of events

Grupo de Astrofísica
Universidad Autónoma de Madrid

- Initially, the universe was fully ionised and optically thick due to electron scattering.
- Matter and radiation strongly interacted → Black Body distribution of radiation.
- Eventually, the Universe cooled sufficiently for atomic H to form → 3000 K , $t = 10^5$ yr , $z = 1000$
- Radiation decoupled from matter.

Temperature and redshift

Non-relativistic matter

$$\mathrm{d}E = -P\mathrm{d}V;$$

$$\dot{E} = \left(\rho_m c^2 + \frac{3}{2}\frac{\rho_m k_B T_m}{m_p}\right) a^3;$$

$$P = n k_B T_m = \frac{\rho_m k_B T_m}{m_p},$$

$$T_m = T_{0m}\left(\frac{a_0}{a}\right)^2 = T_{0m}(1+z)^2.$$

Relativistic matter and Radiation

$$< u > \equiv \rho_r c^2 = \sigma_r T_r^4,$$

photon density decreases with a^3 but photons loose energy due to cosmological red-shifting (extra factor of $1+z$), so

$$\rho_r \propto (1+z)^4,$$

$$T_r = T_{0r}(1+z).$$

UNIVERSIDAD AUTONOMA DE MADRID

Radiation-Matter equality

Grupo de Astrofísica
Universidad Autónoma de Madrid

The thermal history of the Universe reveals a change from *radiation* to *matter* dominated.

- Energy density (matter) ~ $\rho_m c^2$
- $\rho_m \sim 1/a^3$
- # density (photons) ~ $1/a^3$

But, the red-shifting means that energy per photon ~ $1/a$. Thus, energy density (radiation) ~ $1/a^4$

$$\frac{\rho_r}{\rho_m} = \frac{\rho_{0r}}{\rho_{0m}}(1+z),$$

Energy density of radiation drops more quickly than matter as <u>scale factor</u> increases.

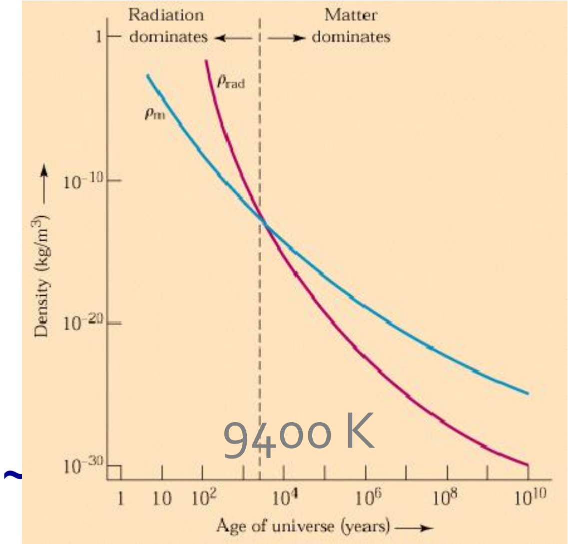

The time when radiation and matter contributed equally in the Universe occurred at:

z_{eq} = 3454 when temperature was about 9400 K

UAM UNIVERSIDAD AUTONOMA DE MADRID

Concordance model

Grupo de Astrofísica
Universidad Autónoma de Madrid

Component	Property
photons	$\Omega_{\gamma,0} = 5.0 \times 10^{-5}$
neutrinos	$\Omega_{\nu,0} = 3.4 \times 10^{-5}$
total radiation	$\Omega_{r,0} = 8.4 \times 10^{-5}$
baryonic matter	$\Omega_{\mathrm{bary},0} = 0.04$
nonbaryonic dark matter	$\Omega_{\mathrm{dm},0} = 0.26$
total matter	$\Omega_{m,0} = 0.30$
cosmological constant	$\Omega_{\Lambda,0} \approx 0.70$

Friedmann equation (now including radiation density term and assuming flat curvature)

$$\frac{da}{dt} = H_0 \left[\frac{\Omega_{r,0}}{a(t)^2} + \frac{\Omega_{m,0}}{a(t)} + \Omega_{\Lambda,0} a(t)^2 \right]^{1/2} .$$

Since the three components have different dependences on scale factor, there are long stretches of history when one component dominates. **First radiation, then matter, then Λ…**

- matter and radiation energy densities equal → $a_{rm} = 0.00029$ *(z=3454)*
- Λ and matter energy densities equal → $a_{m\Lambda} = 0.75$ *(z=0.33)*

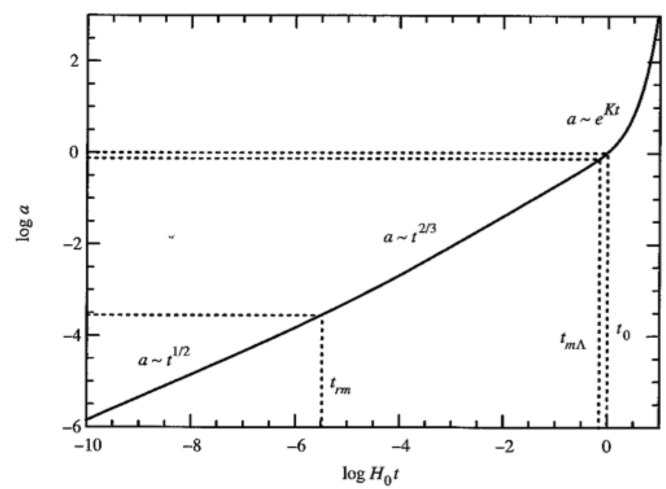

Photon - Baryon Number Density Ratio

- The present density of baryons is:

$$n_{0b} = \frac{\rho_{0b}}{m_p} \simeq 1.12 \times 10^{-5}\Omega_{0b}h^2\text{cm}^{-3}.$$

- Photon's obey Bose-Einstein statistics and integrating over the applicable distribution function give their number density:

- $$n_{0\gamma} = \frac{2\zeta(3)}{\pi^2}\left(\frac{k_B T_{0r}}{\hbar c}\right)^3 \simeq 420\text{cm}^{-3}$$ mostly CMB (only 10% from starlight)

- The photon-baryon ratio, η, (with $(\Omega_{0b}h^2)$ = 0.024 (WMAP CMB values))

$$\eta_0^{-1} = \frac{n_{0b}}{n_{0\gamma}} \simeq 3.75 \times 10^7(\Omega_{0b}h^2)^{-1}. \quad = 1.6 \times 10^9$$

- There are far more photons than baryons in the present Universe

The recombination era

- This is the epoch when charged electrons and protons first became bound to form neutral hydrogen atoms.
- At **recombination**, the mean free path of a photon rapidly goes from being very short to essentially infinite as the probability for scattering off an electron becomes negligible.

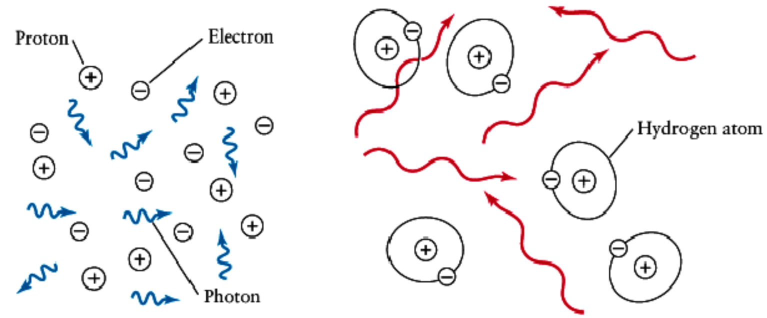

a Before recombination   b After recombination

This epoch is referred to as the **surface of last scattering** or the time of **decoupling** – when radiation and matter became decoupled.

The surface of last scattering

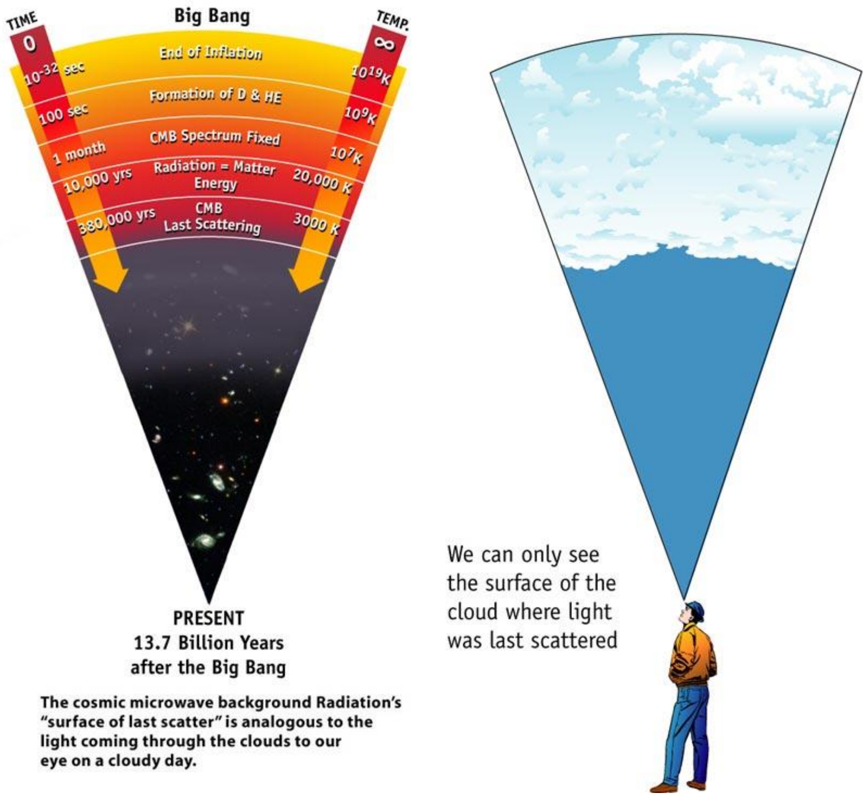

The cosmic microwave background Radiation's "surface of last scatter" is analogous to the light coming through the clouds to our eye on a cloudy day.

Matter-radiation decoupling

n↔p decoupling (A)

n free decay (A-B)

D formation (B)

n↔p equilibrium

n free decay

exact calculation

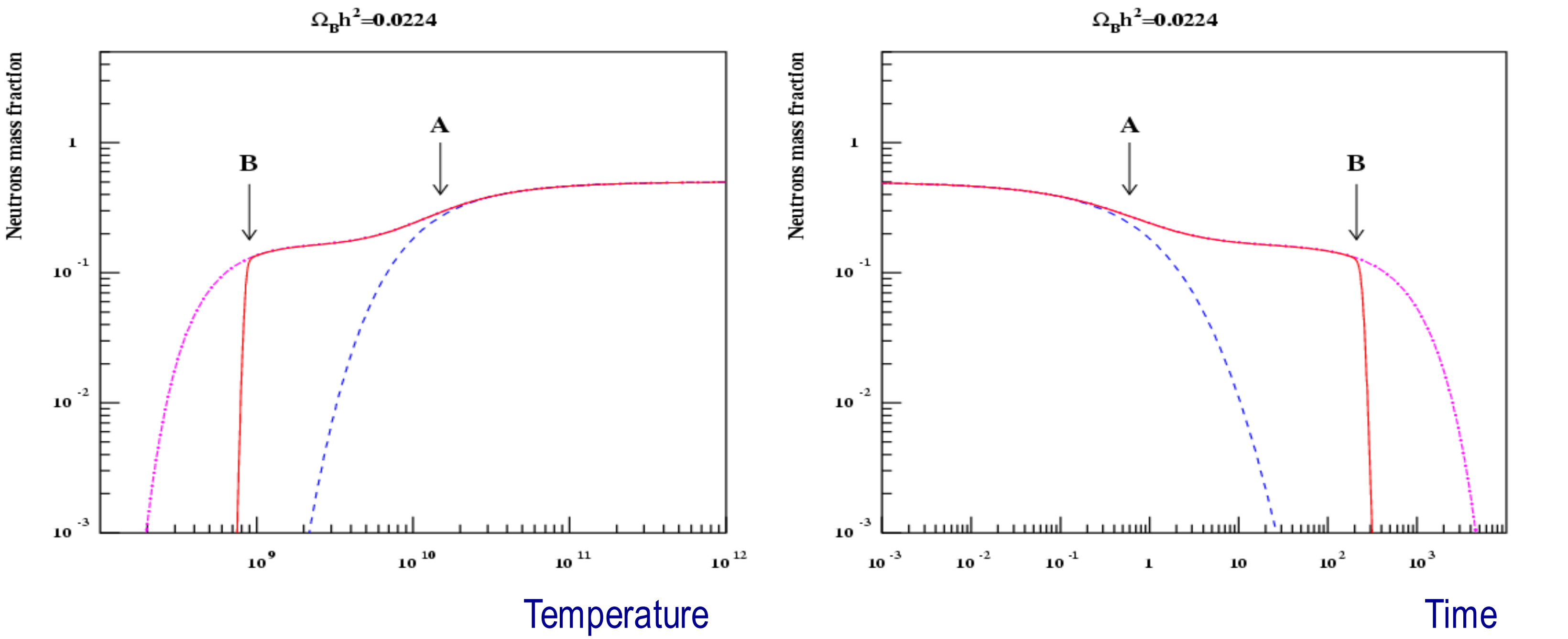

Observational tests of the Standard Big Bang cosmology model

- **S**tandard **B**ig **B**ang **N**ucleosynthesis (SBBN)
  - Calculated ^{4}He, D, ^{3}He, ^{7}Li primordial abundances as functions of the baryonic density η (or $\Omega_b h^2$)
- Spectroscopy
  - Observed ^{4}He, D, ^{3}He, ^{7}Li abundances as functions of metallicity $\rightarrow$ primordial abundances
- Anisotropies in the Cosmic Microwave Background radiation
  - WMAP gives η with $\approx$ 3% precision
- Experimental physics :
  - Number of neutrino families $N_\nu = 2.9840 \pm 0.0082$ (LEP)
  - Nuclear reaction rates and neutron lifetime

Big Bang nucleosynthesis

- In the first three minutes, the Universe was hot enough for nuclear reactions to take place.
- Protons and neutrons formed ^2H (deuterium), ^3He and ^4He.
- ^4He is most stable and, within 3 minutes, made up 25% of the Universe.

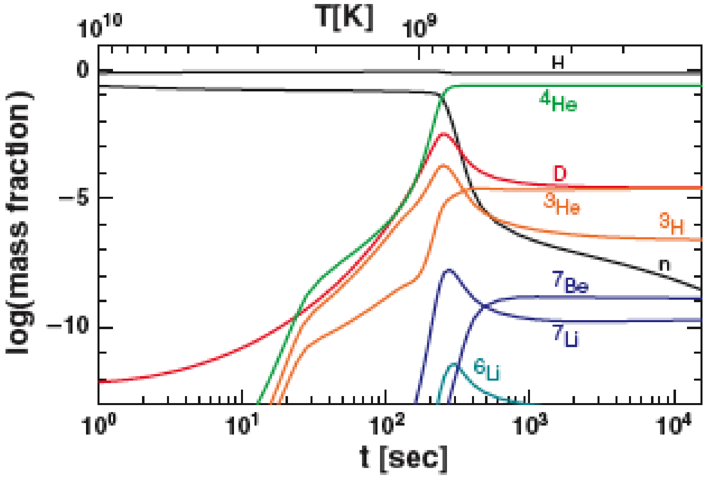

UNIVERSIDAD AUTONOMA DE MADRID

Primordial nucleosynthesis

Grupo de Astrofísica
Universidad Autónoma de Madrid

- Protons are somewhat lighter than neutrons:
  - m_p= 938.3 MeV
  - m_n= 939.6 MeV Δm= 1.3 MeV
- Free neutron decay $n \rightarrow p + e^-$ with a half life of 940 s
- Bound e^- in nuclei are stable.
- At high T, $N_p \approx N_n$ since the mass-energy difference is negligible w.r.t. kT, so
  - $n \leftrightarrows p + \bar{e}^- + \nu_e$ (+0.8 MeV) as the main process
- But, when $\Uparrow$ $kT \approx$ 0.8 MeV, neutrons can convert to protons but the inverse reaction is not possible
- Protons begin to outnumber neutrons by a factor:

$$\frac{N_p}{N_n} \sim e^{(Dm/kT)} \sim e^{(1.3/0.8)} \sim 5$$

The formation of ^4He

- Protons and neutrons combine to build up more complex nuclei.
- Densities are still too low for many body collisions, so reactions start as:

$$p + n \rightarrow {}^2D + \gamma$$
$${}^2D + n \rightarrow {}^3T + \gamma$$
$${}^2D + p \rightarrow {}^3He + \gamma$$
$${}^2D + {}^2D \rightarrow {}^3He + n$$
$${}^3He + n \rightarrow \mathbf{{}^4He + \gamma}$$
$${}^3He + n \rightarrow {}^3T + p$$
$${}^3T + p \rightarrow \mathbf{{}^4He + \gamma}$$

- ^2H is very reactive, so most neutrons in ^2H will end up in **^4He,** with traces of D, ^3He, ^7Li, …

The mass fraction of ^{4}He

- Mass fraction in ^{4}He is:

$$Y = 2n_n/(n_p+n_n) = 2(n_n/n_p)(1+n_n/n_p)^{-1}$$

- Proton to neutron ratio set at 1/5 which yields Y ~ 0.3.
- The actual value is somewhat lower because D forming reaction is suppressed by the high photon - to - baryon ratio.
- In these terms, the mass fraction of ^{4}He is:

$$\begin{aligned} Y = (0.230) + (0.0011)\ln\left(\frac{10^{10} n_B}{n_\gamma}\right) \\ + (0.013)(N_L - 3) \\ + (0.014)(t_{1/2} - 10.6\ \mathrm{min}) \end{aligned}$$

- N_L is the number of light particles, like neutrinos. The best model fit for a relativistic gas (dominated by neutrino motions) is 3.

Primordial nucleosynthesis with η

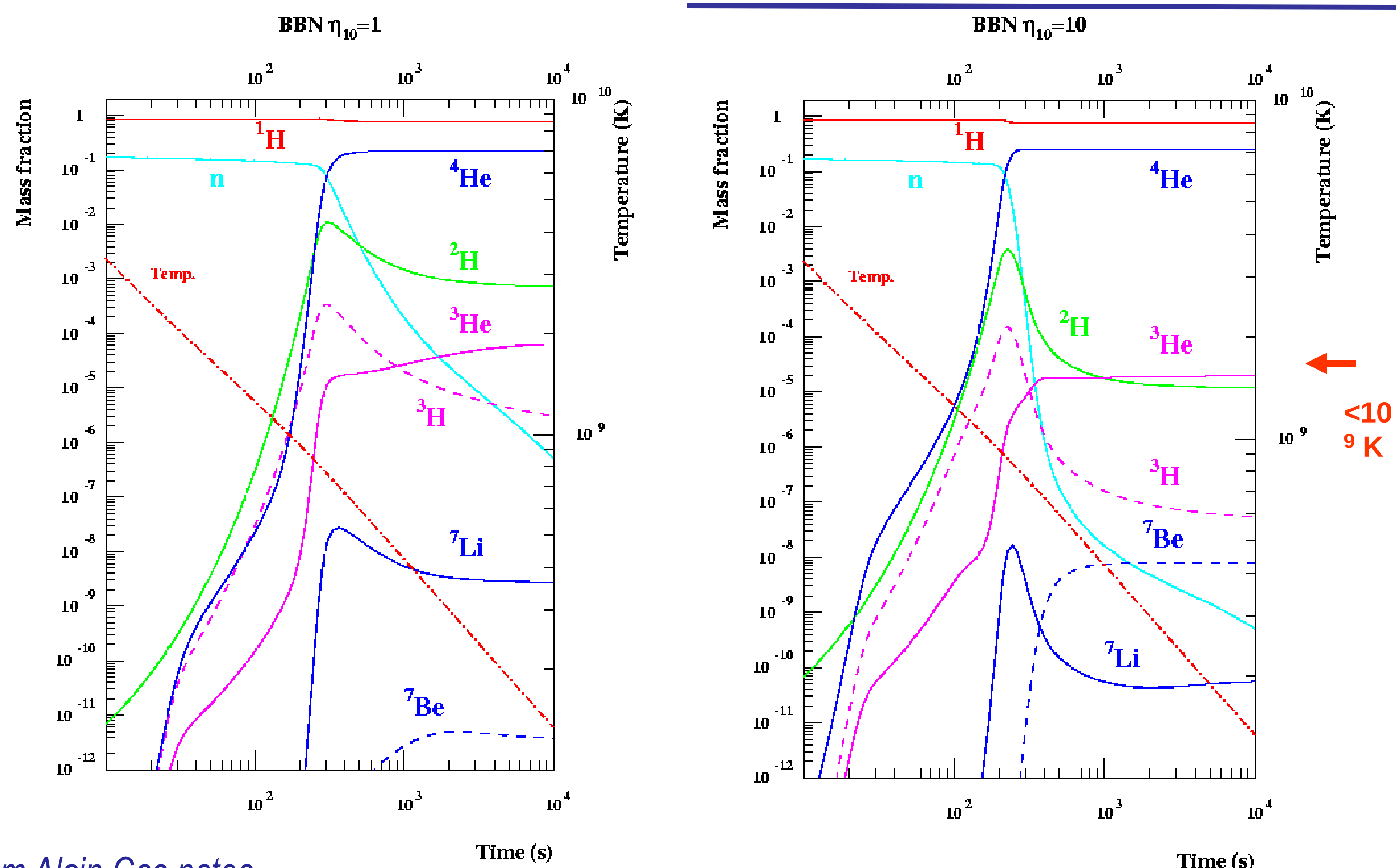

From Alain Coc notes.

Primordial abundances as "baryometers"

- Not only the abundances of primordial He but also those of the rest of elements produced as result of the BB, depend on the baryon to photon ratio.
- The abundances of ^{4}He, ^{2}D, ^{3}He, ^{7}Li have to converge to a single value in the abundance *vs* baryon-to-photon ratio.
- For the SBBN model to be confirmed these values should also converge to the model predicted ones.

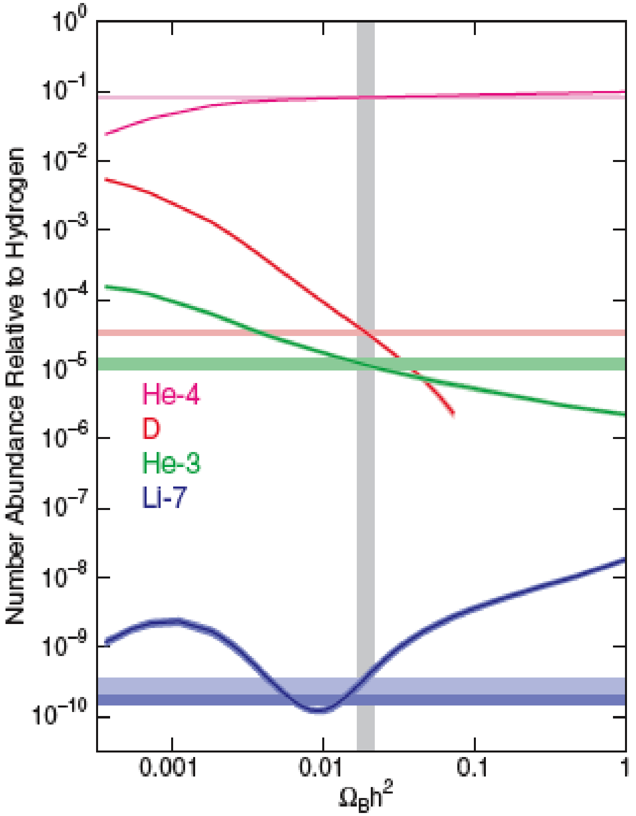

Reaction rates

Origin of reaction rates

Theoretical:

• $n \leftrightarrow p$: *[Dicus et al. (1982), Lopez & Turner (1999)]*

• ^{1}H$(n,\gamma)^2$H : Two nucleons effective field theory *[Chen & Savage (1999)]*

Experimental :

• Compilation *[Descouvemont, Adahchour, Angulo, Coc & Vangioni-Flam (2004)]*

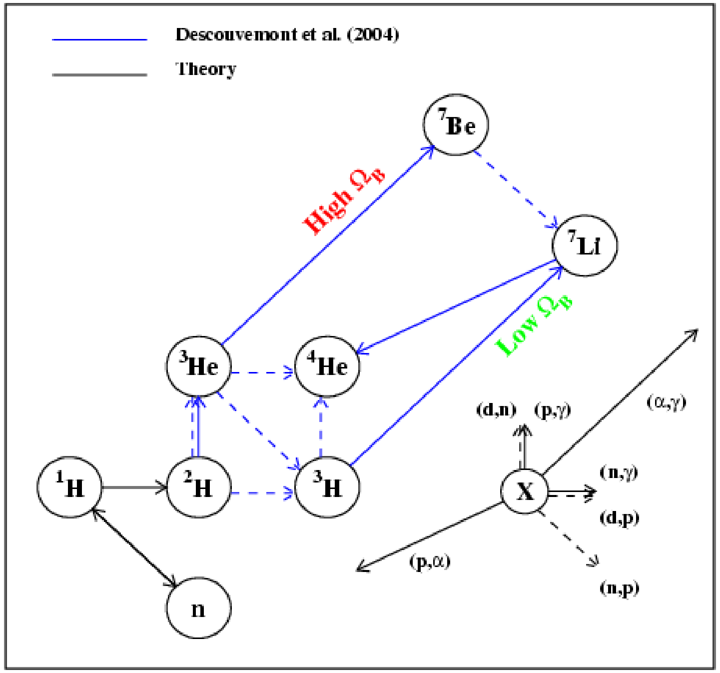

From Alain Coc notes.

Primordial abundance measurements

Primordial abundances :

- Observe a set of primitive objects born when the Universe was young
  - ^{4}**He** in H II (ionized H) regions of blue compact galaxies
  - ^{3}**He** in H II regions of *our* Galaxy (?)
  - **D** in remote cosmological clouds (i.e. at high redshift) on the line of sight of quasars
  - ^{7}**Li** at the surface of low metallicity stars in the halo of our Galaxy
- Extrapolate to zero metallicity : Fe/H, O/H, Si/H,…. $\rightarrow$ 0

Primordial helium measurements

1. Take an emission line spectrum
2. Measure the temperatute, T_e
3. Measure the density, n_e
4. Calculate (theoretical) emissivities
5. Convert relative eission line flux measurements to relative abundances
6. Plot a regression of He/H vs O/H, N/H, S/H … and explapolate bak to zero abundance

Typical object for Y_p determination

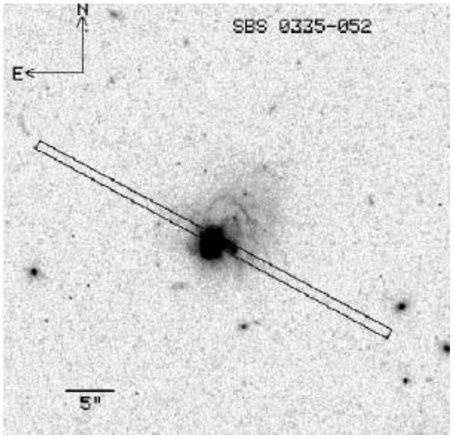

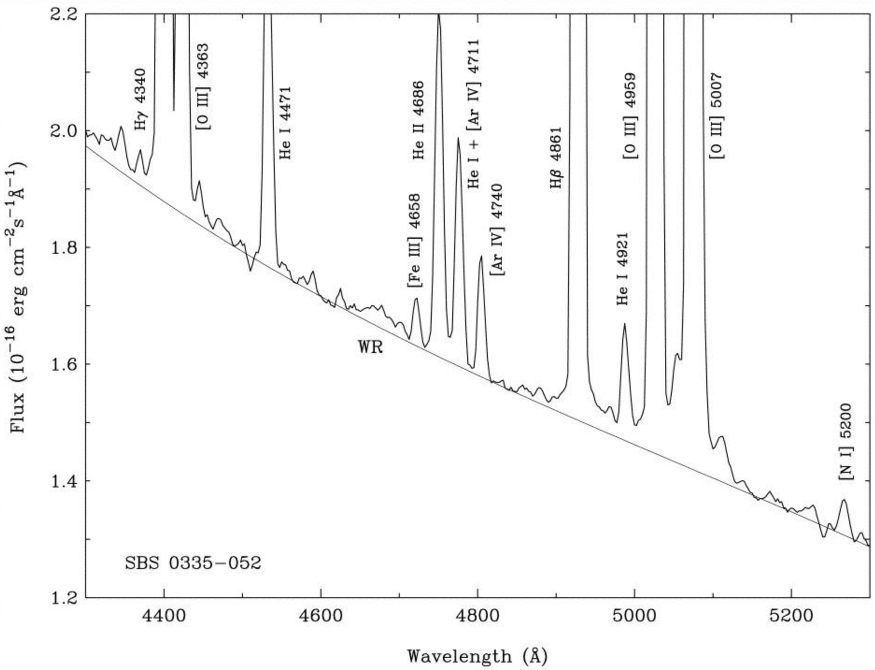

Izotov et al. 1999, 527, 757

Primordial He from O/H and N/H abundances

Pagel et al 1992, MNRAS, 255, 325

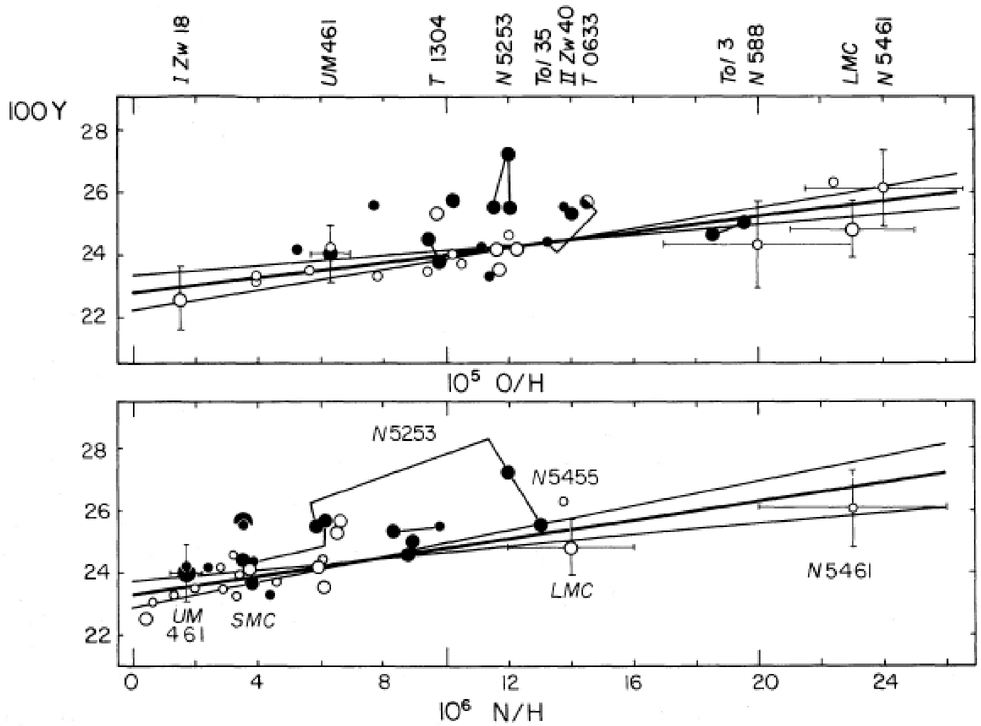

Yp = 0.228 ± 0. 005

Figure 7. Regressions of helium against oxygen and nitrogen abundances for objects with definite detections of broad WR features (filled circles) and without definite detections (open circles). Maximum-likelihood regression lines are shown for the latter category, with alternatives equivalent to $\pm 1\sigma$ limits. Larger and smaller circles represent higher and lower weights, respectively, and a few typical error bars are shown.

"there may be additional local sources of both helium and nitrogen in the form of winds from Wolf-Rayet stars"

The primordial He abundance

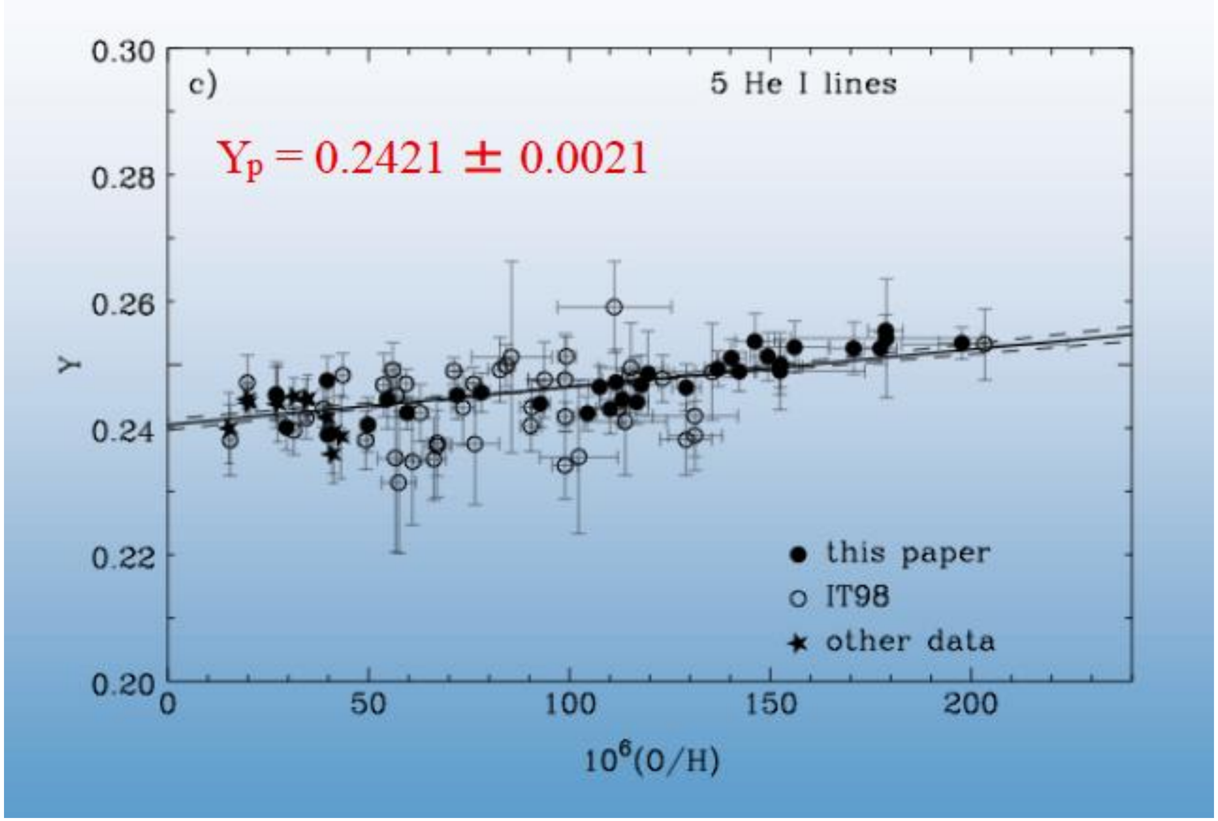

Izotov & Thuan 2004, 602, 200

The primordial helium abundance Y_p

$Y_{p(WMAP)} = 0.2485 \pm 0.0002$

Aver et al. 2013, JCAP, 11, 17

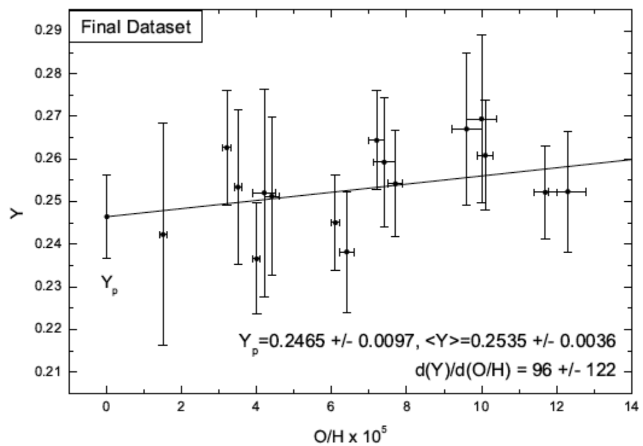

Figure 5. Helium abundance (mass fraction) versus oxygen to hydrogen ratio regression calculating the primordial helium abundance.

Aver et al. 2015, JCAP, 07, 011
adding the HeI 10830 A line

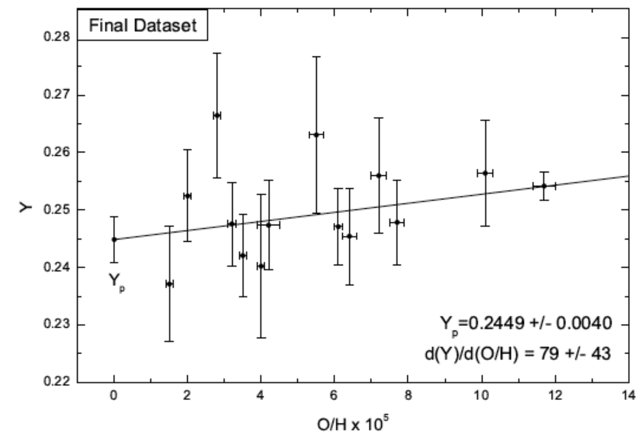

Figure 6. Helium abundance (mass fraction) versus oxygen to hydrogen ratio regression calculating the primordial helium abundance.

$Y_p = 0.2465 \pm 0.0097$

$Y_p = 0.2449 \pm 0.0040$

The primordial helium through the years …

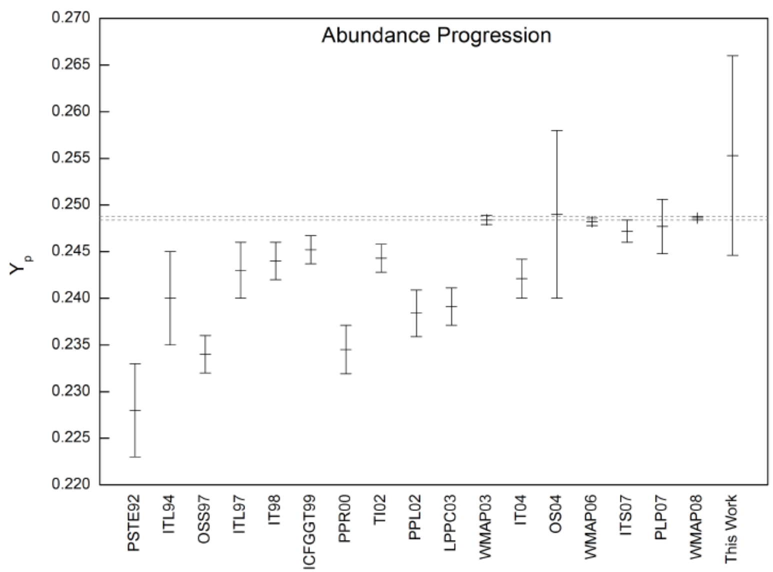

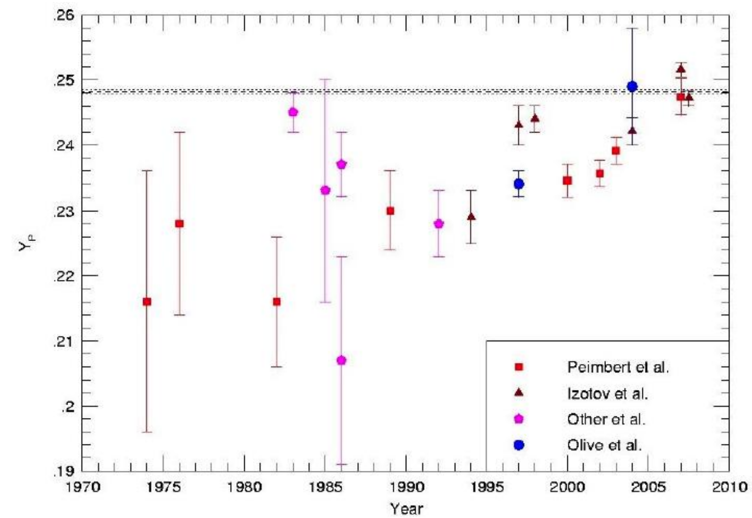

Uncertainty sources

TABLE 7

Error Budget in the Y_p(sample) Determination

Problem	Estimated Error
Collisional excitation of the H I lines	±0.0015[a]
Temperature structure	±0.0010[b]
$O(\Delta Y/\Delta O)$ correction	±0.0010[a]
Recombination coefficients of the He I lines	±0.0010[a]
Collisional excitation of the He I lines	±0.0007[b]
Underlying absorption in the He I lines	±0.0007[b]
Reddening correction	±0.0007[a]
Recombination coefficients of the H I lines	±0.0005[a]
Underlying absorption in the H I lines	±0.0005[b]
Helium ionization correction factor	±0.0005[b]
Density structure	±0.0005[b]
Optical depth of the He I triplet lines	±0.0005[b]
He I and H I line intensities	±0.0005[b]

[a] Systematic error.
[b] Statistical error.

Peimbert, Luridiana & Peimbert 2007

Using Sulphur as metallicity tracer

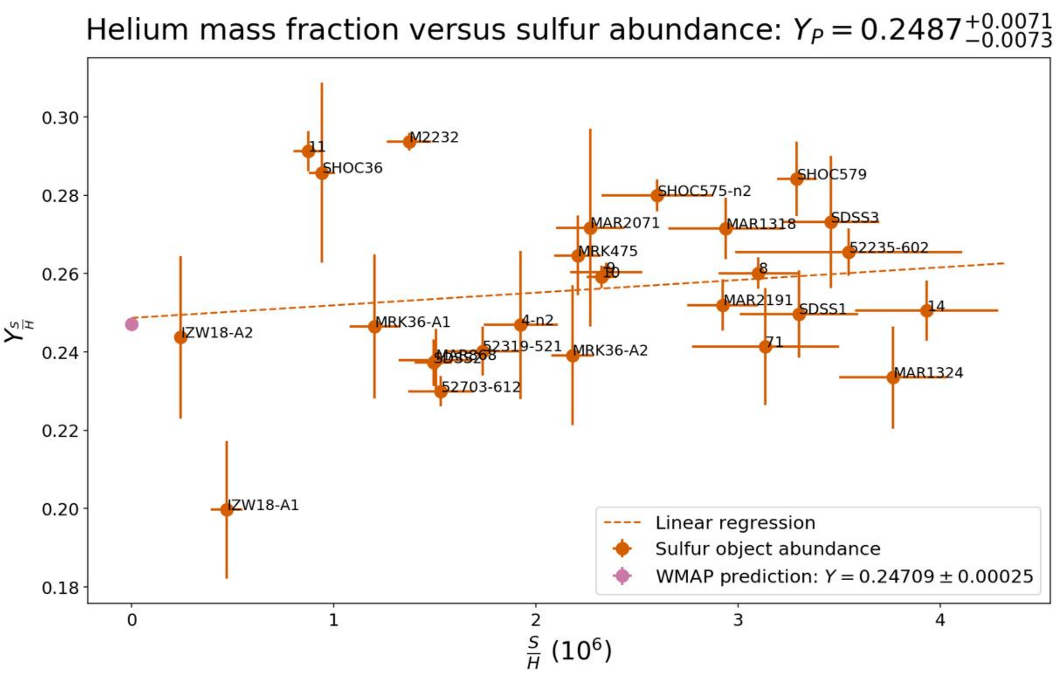

Fernández et al. 2018, MNRAS, 478, 5301

The PHLEK Survey:

Hsyu et al. 2020, ApJ, 896, 77

- Keck NIRSPEC and Keck NIRES spectroscopy of sixteen metal-poor galaxies that have pre-existing optical observations.
- The near-infrared (NIR) spectroscopy specifically targets the He I λ10830 Å emission line, due to its sensitivity to the physical conditions of the gas in H II regions
- The NIR observations are combined with data from the literature.
- They derive a primordial helium mass fraction of
  - $Y_P = 0.2436^{+0.0039}_{-0.0039}$

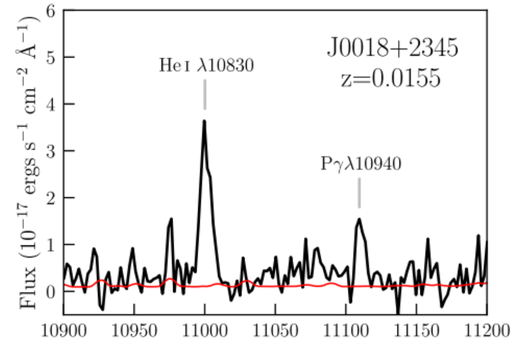

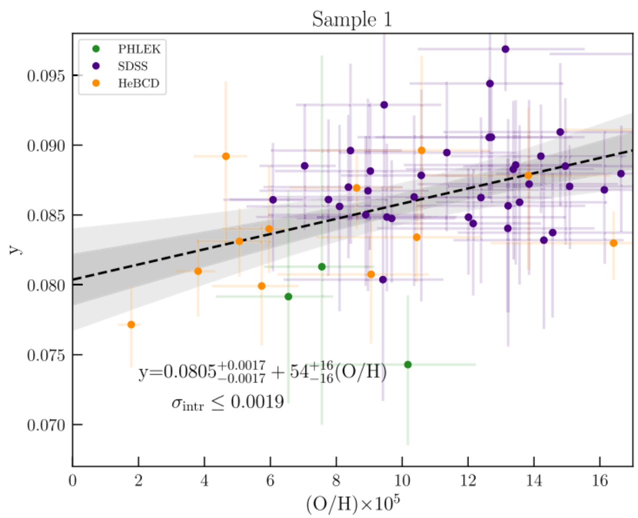

Using a large SDSS sample

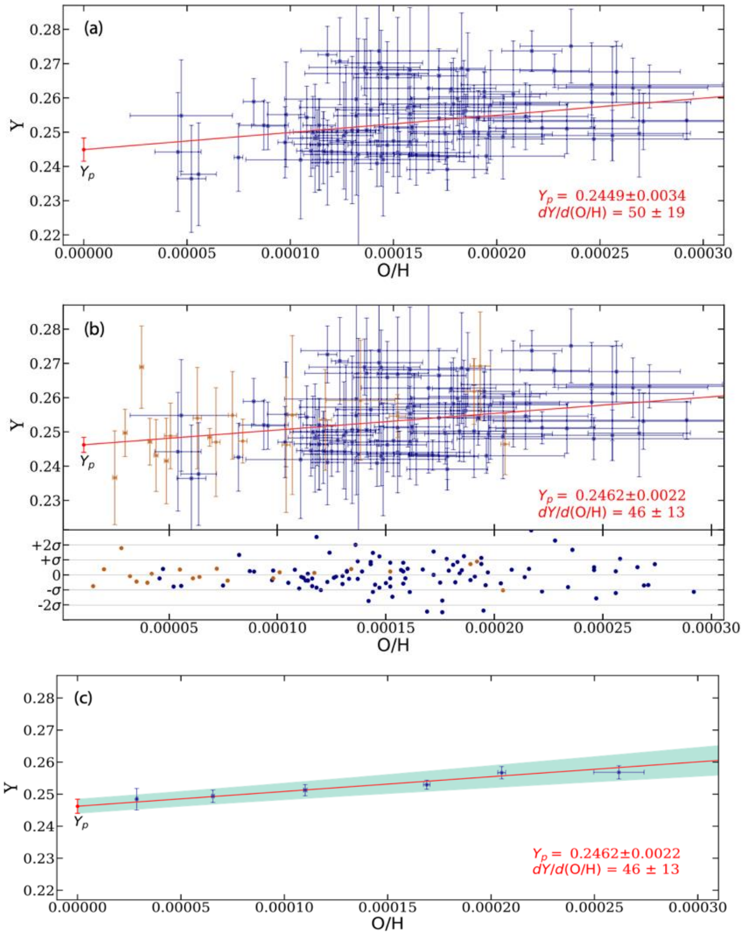

- A sample of 100 H II regions collected from the Sloan Digital Sky Survey.
- The final analysed sample consists of our sample and HeBCD data base from Izotov et al. (2007).
- The value obtained is $Y_p = 0.2462 \pm 0.0022$.
- This should be compared with the Planck result:
  - $Y_{planck,\,p} = 0.2471 \pm 0.0003$

Kurichin et al. 2021, MNRAS, 502, 3045

Primordial helium abundance from observations of the intergalactic medium.

Cooke et al., 2018, Nature Astronomy, 2, 957

- A determination of the primordial helium abundance based on a near-pristine intergalactic gas cloud that is seen in absorption against the light of a background quasar.
- This gas cloud is at z_{abs} = 1.724, has a metal content around 100 times less than that of the Sun, and at least 30% less metal content than the most metal-poor HII region currently known where a determination of the primordial helium abundance is possible.
- that the helium abundance of this intergalactic gas cloud is Y =0.25 0-0.025+0.033 , which agrees with the standard model primordial value8-10, Y_P = 0.24672 ± 0.00017

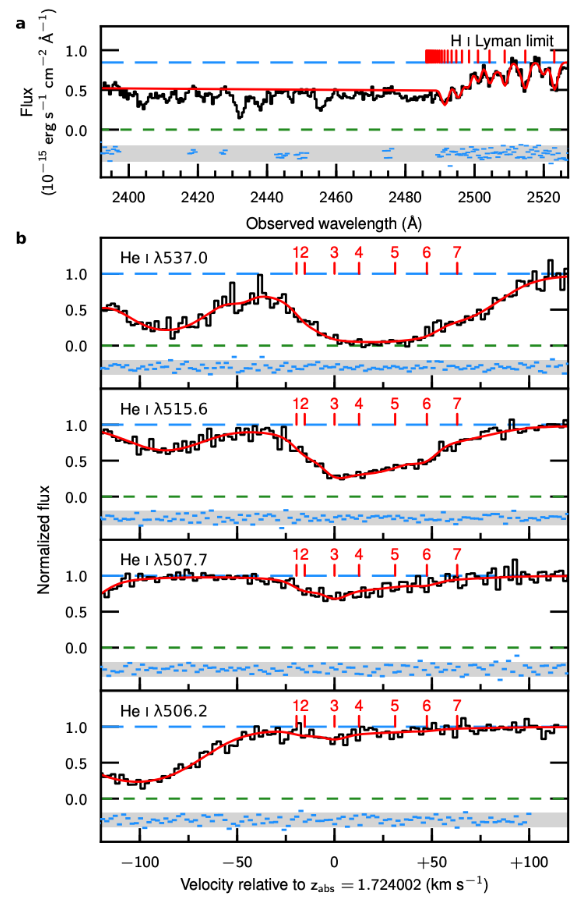

The primordial deuterium abundance

- Since ^{2}D is strongly dependent on the baryon density, it is an excellent “baryometer”.
- There are no known astrophysical sources for deuterium production and thus **all deuterium must be of primordial origin.**
- But the monotonic decrease in the deuterium abundance over time indicates that the galactic chemical evolution affects the interpretation of any local measurements of the deuterium abundance such as in the local ISM, galactic disc, or galactic halo.

Spectra for ²D abundance measurements

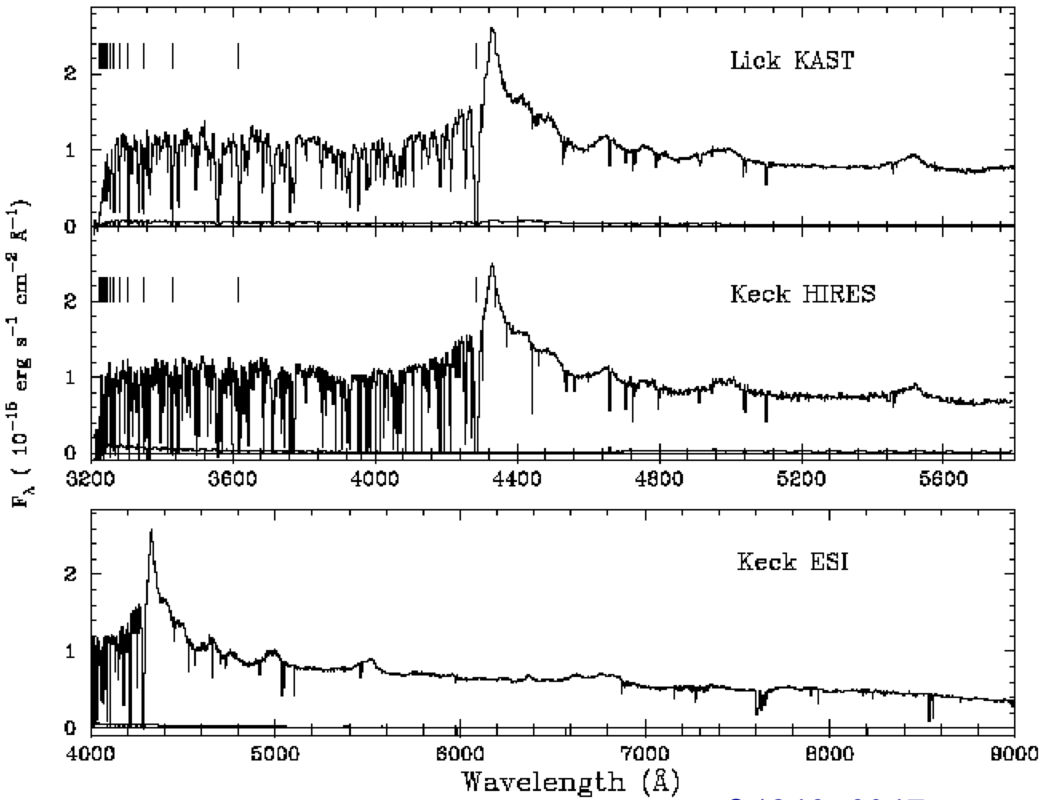

Q1243+3047

Kirkman et al. 2003, ApJS, 149, 1

The derivation of D/H

- D can be measured in IG gas clouds from the Lyman absorption lines in the spectra of distant QSOs.
- D Ly lines are at 82 kms^{-1} to the blue side of their corresponding H Ly line.
- D can be detected in select absorption systems with very simple velocity structure and high HI column density (> 10^{17} cm^{-2}).
- For high redshifts (z> 2.5) the Ly series is redshifted into the optical and the lines become accessible to large ground-based telescopes.
- The Ly absorption lines of DI and HI, plus the Ly continuum absorption of HI, constrain the column densities of DI and HI and provide the DI/HI ratio.
- The time to reach ionisation equilibrium for H and D is short (~10^5 yr) and in the IGM we can assume DI/DH = D/H.

D/H from the most metal poor DLAs

$\langle \log (D/H)_p \rangle = -4.55 \pm 0.03$
$\Omega_{b,0}h^2(\text{BBN}) = 0.0213 \pm 0.0010$

Pettini et al. 2008, MNRAS, 391, 1499

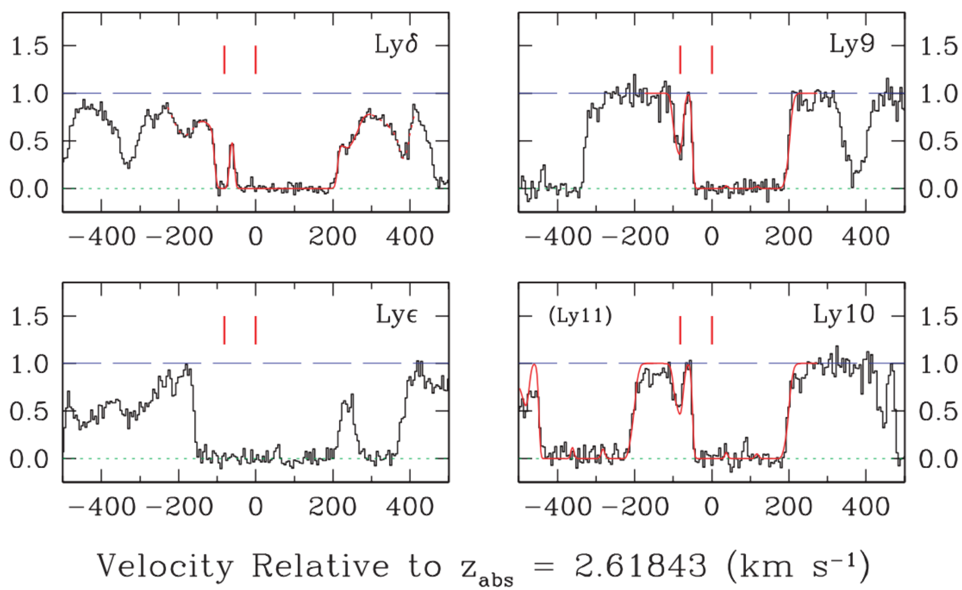

Observed profiles (black histograms) and fitted Voigt profiles (continuous red lines) of absorption lines in the Lyman series of the z_{abs} = 2.61843 DLA in Q0913+072. The y-axes of the plots show relative intensity. The two vertical tick marks in each panel indicate the expected locations of the main absorption component of the DLA in, respectively, H I (at v = 0 km s^{-1} in the plots) and D I (at v = −81.6 km s^{-1}).

D/H from the most metal poor DLAs

Cooke et al. 2014, ApJ, 781, 31

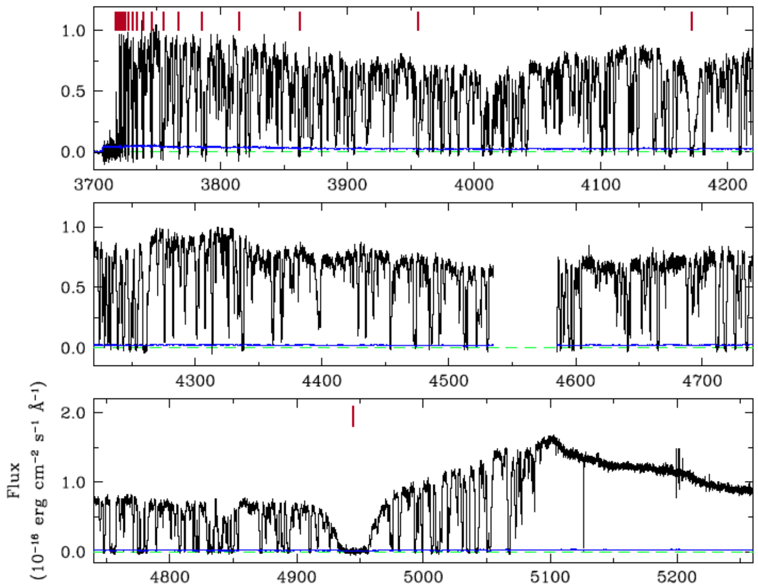

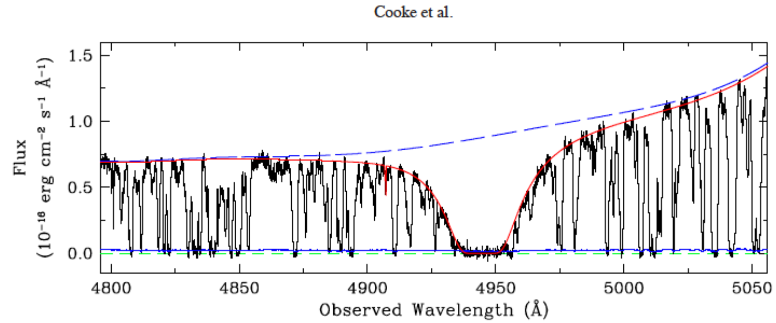

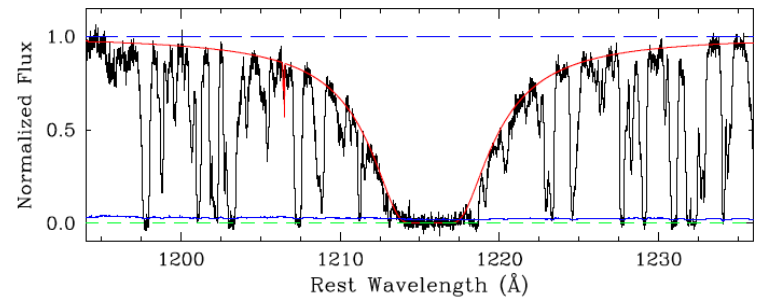

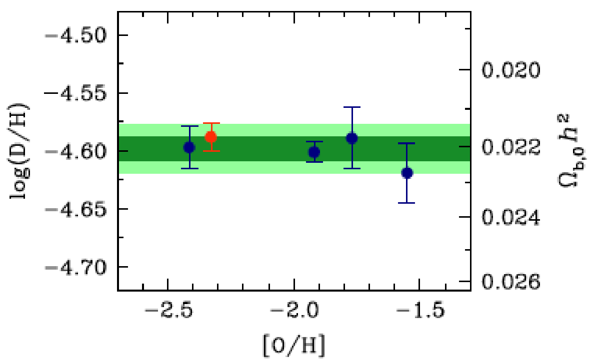

$D/H_p = (2.53 \pm 0.04)\ 10^{-5}$

A new precise determination

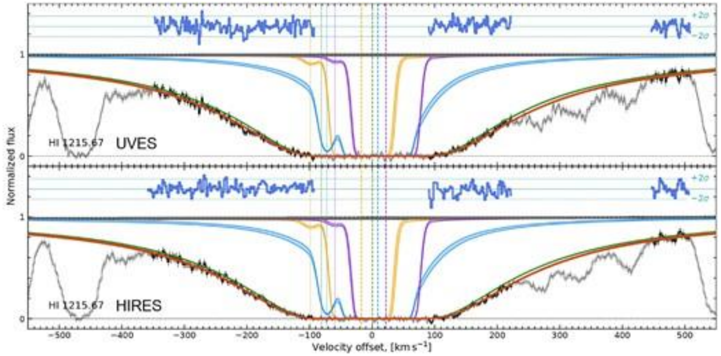

Kislitsyn et al. 2024, MNRAS528, 4068

- D I absorption lines in a metal-poor sub-Damped Lyman-α system at $z_{abs} = 3.42$ towards the quasar SDSS J133254.51+005250.6.
- Derived deuterium value of (D I/H I) = −4.622 ± 0.014.
- Incorporating all prior measurements, the best estimate of the primordial deuterium abundance is constrained as: $(D/H)pr = (2.533 \pm 0.024) \times 10^{-5}$.
- This represents a 5 per cent improvement in precision over previous studies and reveals a moderate tension with the expectation from the standard model (≈2.2σ).
- This discrepancy underscores the importance of further measurements in the pursuit of new physics.

The Deuterium abundance in the solar bubble

- These techniques can also be applied to the local ISM by using UV .
- *Wood et al (2004)* from FUSE data find:

  D/H = $(1.56 \pm 0.04)\ 10^{-5}$

  for the local bubble and

  D/H = $(0.85 \pm 0.09)\ 10^{-5}$ for the local galactic disc.
- This lower value for the disc could be due to variable astration and/or incomplete mixing with the ISM or depletion onto dust grains.

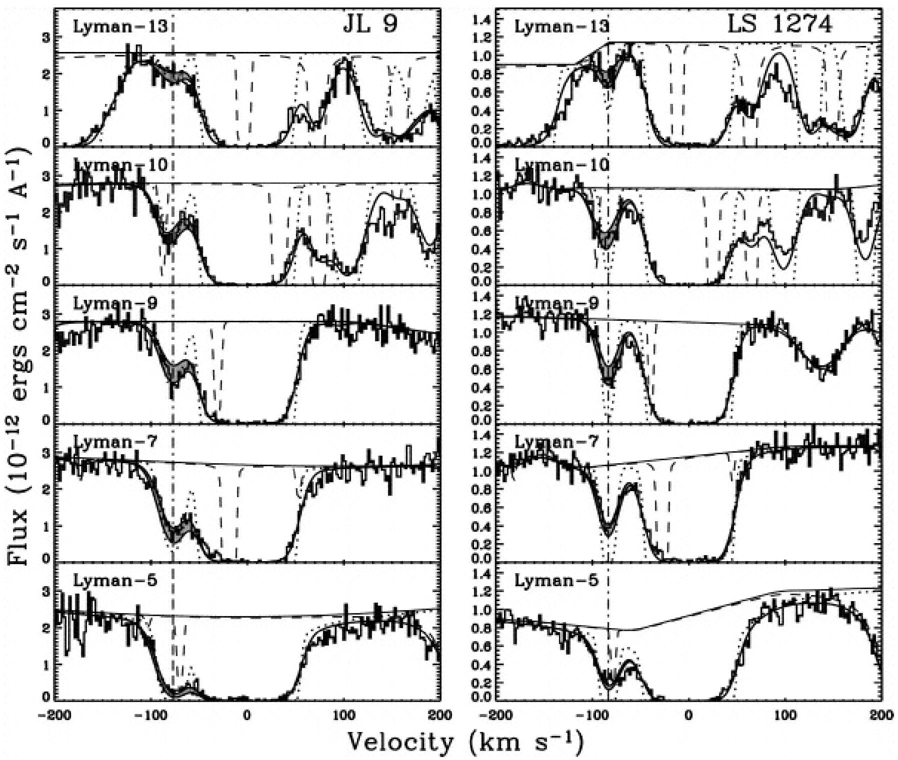

Wood et al. 2004, ApJ, 609, 838

The galactic Deuterium

- D abundances can also be found from the 327 MHz hyperfine transition.
- Rogers et al (2007) find

  $D/H = (2.1 \pm 0.7)\ 10^{-5}$

  for the region of the galactic anticenter.
- This value lower than the primordial one is ascribed to depletion onto dust grains.

Rogers et al. 2007, AJ, 133, 1625

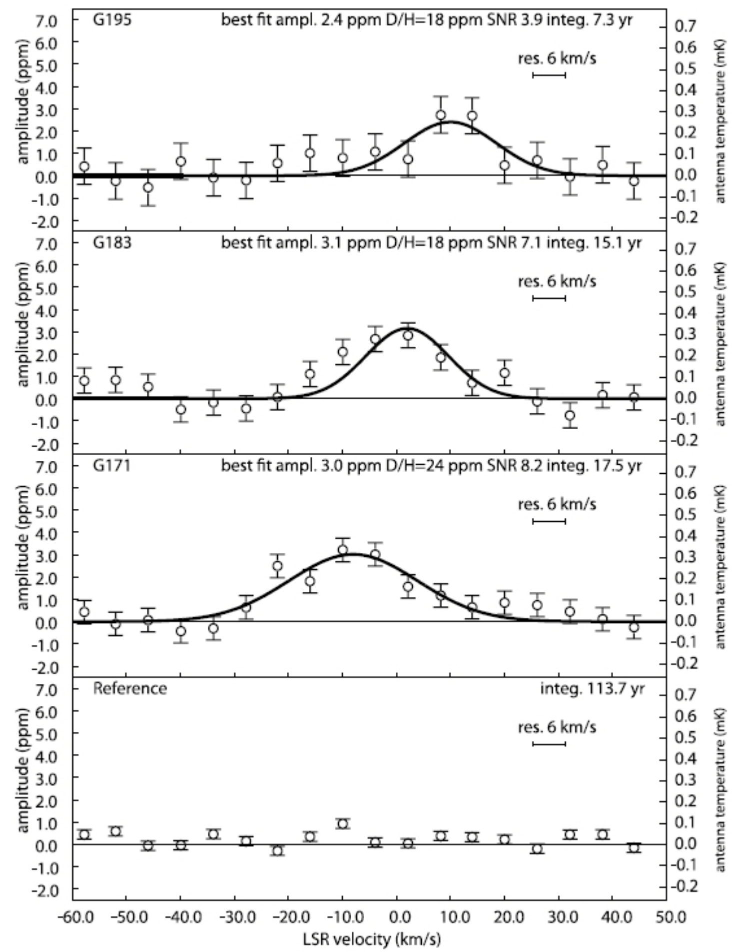

Lithium nucleosynthesis

- Nuclei of mass number 7 are in the form of stable ^{7}Li, but also as radioactive ^{7}Be.
- In its neutral form, ^{7}Be decays via electron capture with a half-life of 53 days.
- In the early universe, however, the decay is delayed until the universe is cool enough that ^{7}Be can finally capture an electron at z 30000 [82], shortly before hydrogen recombination! Thus, ^{7}Be decays long after the 3 min timescale of BBN.
- After recombination, all mass-7 takes the form of ^{7}Li.
- ^{7}Li/H theoretical predictions sum both mass-7 isotopes.

$\boxed{^4He + {}^3H \rightarrow {}^7Li + \gamma}$

$\boxed{^4He + {}^3He \rightarrow {}^7Be + \gamma}$ $\boxed{^7Be + n \rightarrow {}^7Li + p}$ $\boxed{^7Li + p \rightarrow 2\ {}^4He}$

The "Lithium deep"

- ^{7}Li production dominates at low η, while ^{7}Be dominates at high η, leading to the characteristic "lithium dip" versus baryon density in the Schramm plot.

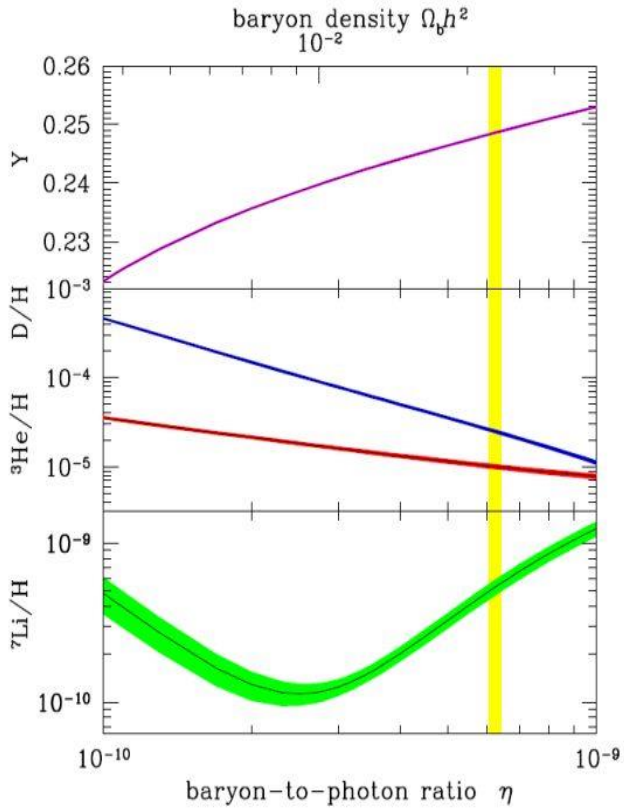

Lithium abundance determination

- Lithium is measured in the atmospheres of metal poor halo stars (Pop II) in our Galaxy.
- Due to convective motions, surface material in stars can be dragged down to the inner regions where it is rapidly destroyed.
- But the hottest of these stars have very thin convective zones and these can be used to measure unprocessed ^{7}Li.

The "Spite plateau"

- For a sample of halo stars Li/H is nearly independent of Fe/H → this flat trend is known as the **"Spite plateau"**
- But heavy elements such as iron ("metals") increase with time as Galactic nucleosynthesis proceeds and matter cycles in and out of stars.
- Thus, the Spite plateau indicates that most halo star lithium is uncorrelated with Galactic nucleosynthesis and hence, **lithium is primordial.**

Asplund et al. 2006

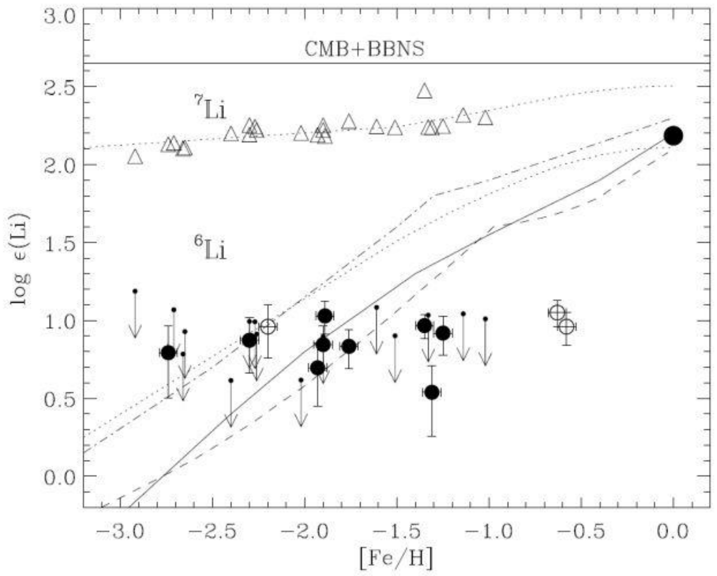

$$\frac{Li}{H} = \left(1.23^{+0.68}_{-0.32}\right)10^{-10}$$

The Lithium discrepancy problem

- Using the CMB primordial abundances values in SBBN (thus removing the only free parameter in the standard theory), we can compute likelihoods for all the light elements.
- The spectacular agreement between observations links z ~ 3 abundance measurement with $z \sim 1000$ CMB data and represents a triumph of the hot big bang cosmology.
- Also, ^{4}He predictions are in good agreement with observations.
- For ^{7}Li, the BBN+WMAP predictions and the measured primordial abundance **completely disagree**: the predictions are substantially higher than the observations.
- The **discrepancy** is a factor

  $\mathrm{Li(BBN+WMAP)} / \mathrm{Li_{obs}} = 2.4-4.3$

  representing a 4.2−5.3 σ discrepancy.

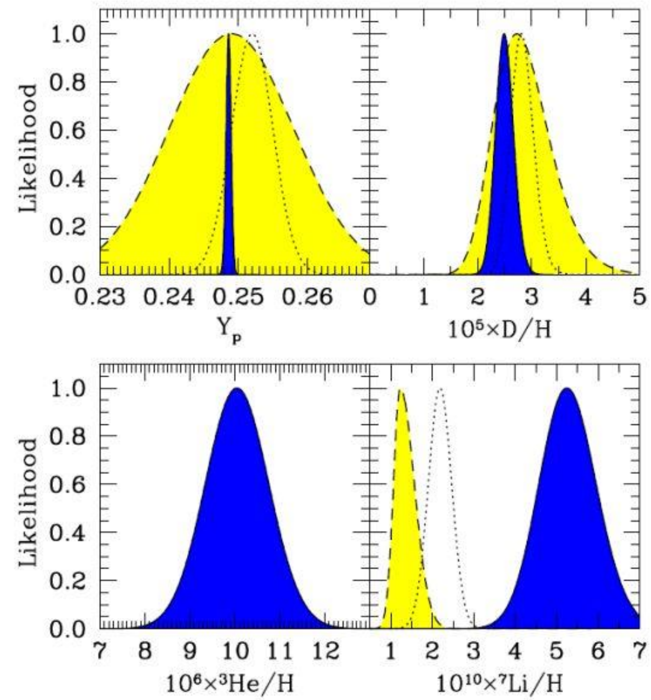

Possible solutions to the Lithium discrepancy

- **Astrophysical solutions**
  - Systematic errors in the derivation of abundances in stellar atmospheres, e.g. in the determination of the T scale in models, initial ^{7}Li content etc.
  - The stars have destroyed part of its ^{7}Li … but stars with [Fe/H] ≤ -3 the abundance is even below the Spite plateau and shows large scatter ...
- **Nuclear physics solutions**
  - Uncertainties in the reaction rates for weak and nuclear interactions.
  - Resonances that have eluded experimental detection and are nort constraint experimentally.
- **Solutions beyond the Standard Model**
  - Dark matter decay (via WIMPS).
  - Changes in fundamental constants.
  - Non-standard cosmologies.
  - You name it …

^{3}He abundances

- The evolution of ^{3}He after the BB is very complex
- The interstellar ^{3}He is incorporated into stars and is burnt to ^{4}He (and other elements) even during pre-main sequence evolution in the hotter interiors; it is however preserved in the cooler outer layers.
- Hence, ^{3}He is destroyed in cooler low-mass stars but it is unclear how much of it will return to the interstellar medium.
- It is thought that the net production of ^{3}He will increase with time and therefore with metallicity.
- Observations of ^{3}He are restricted to the Solar System and our Galaxy.
- For our Galaxy a radial gradient of ^{3}He is expected but it is not clearly observed.

The evolution of ^{3}He

Bania et al. 2004, Nature 415, 54

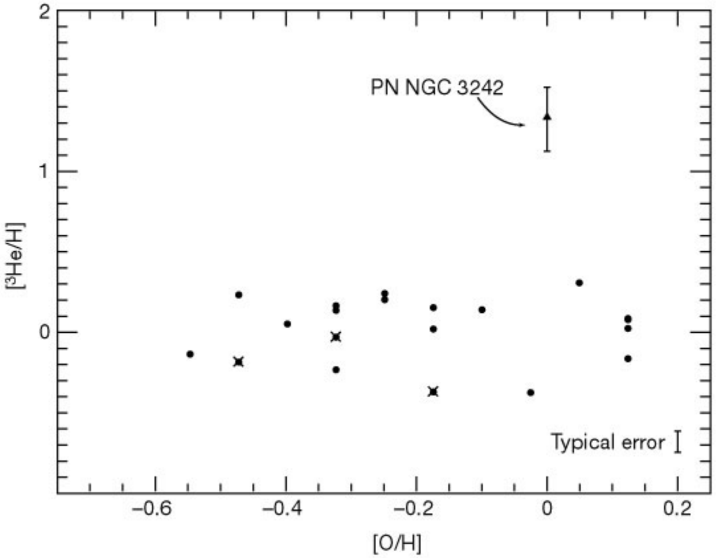

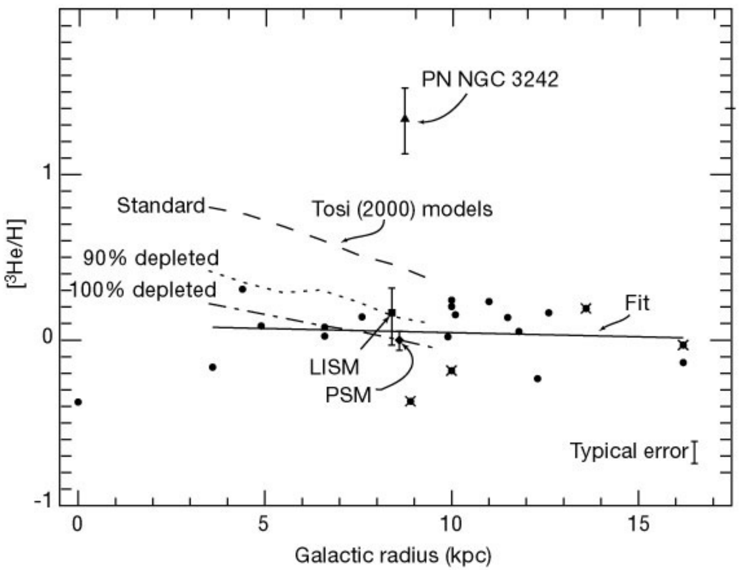

Observations of ^{3}He in HII regions

- ^{3}He abundances in HII regions in the MWG come from measurements of the 8.665 GHz (3.46 cm) spin-flip transition of $^{3}He^{+}$.
- Converting the observed column densities to an abundance ratio relative to hydrogen is not trivial.
- It depends on the density and ionisation structure of each nebula. But large, diffuse HII regions are relatively simple in this respect. They provide the most accurate determinations of the ^{3}He abundance.
- Bania et al. (2002), from a sample of 60 galactic HII regions, set the the lower abundance for ^{3}He at that of a large, diffuse, outer HII region in the MWG: S209 as the primordial ^{3}He value
- $(^{3}He/H)_p = (1.1 \pm 02)\ 10^{-5}$